

Near-Earth object velocity distributions and consequences for the Chicxulub impactor

S. V. Jeffers,^{1,2} S. P. Manley,¹ M. E. Bailey¹[★] and D. J. Asher¹

¹Armagh Observatory, College Hill, Armagh BT61 9DG

²School of Physics and Astronomy, University of St Andrews, St Andrews, Fife KY16 9SS

Accepted 2001 May 25. Received 2001 May 9; in original form 2000 October 27

ABSTRACT

An Öpik-based geometric algorithm is used to compute impact probabilities and velocity distributions for various near-Earth object (NEO) populations. The resulting crater size distributions for the Earth and Moon are calculated by combining these distributions with assumed NEO size distributions and a selection of crater scaling laws. This crater probability distribution indicates that the largest craters on both the Earth and the Moon are dominated by comets. However, from a calculation of the fractional probabilities of iridium deposition, and the velocity distributions at impact of each NEO population, the only realistic possibilities for the Chicxulub impactor are a short-period comet (possibly inactive) or a near-Earth asteroid. For these classes of object, sufficiently large impacts have mean intervals of 100 and 300 Myr respectively, slightly favouring the cometary hypothesis.

Key words: comets: general – Earth – minor planets, asteroids – Moon.

1 INTRODUCTION

The Earth's geological record contains important details of the history of the planet, including evidence of major impact events and abrupt transitions of life associated with mass extinctions. The most famous example is the Cretaceous–Tertiary (K/T) boundary, associated with both an exceptionally large crater, approximately 180 km in diameter, and an anomalously high abundance of iridium and other platinum group elements (Alvarez et al. 1980). Iridium is not found to any significant degree elsewhere in the Earth's crust, owing to its siderophile nature, but it is assumed to be a constituent of undifferentiated bodies such as asteroids and comets. The presence of a large crater together with an anomalous Ir layer at the K/T boundary provides evidence linking impacts with mass extinction. At the same time, the detection of Ir provides evidence of an accretion event.

Not all mass-extinction boundaries show strong Ir signatures, even when associated with large craters. In this respect, the K/T boundary is exceptional, and the lack of significant levels of Ir at other geological boundaries reopens the question whether mass extinctions are mainly caused by impacts or by purely terrestrial processes involving, for example, vulcanism, climate and sea-level changes.

A further important issue for the impact hypothesis is whether the *largest* craters are dominated by comets or asteroids. However, the efficiency of Ir deposition is a strong function of the velocity

and mass of the impactor, both generally higher for comets than for asteroids.

The main purpose of this paper is to determine the impact probabilities and velocity distributions for various near-Earth object (NEO) populations. Resulting from this are detailed crater size distributions and calculations of the fractional probabilities of Ir deposition for each population.

2 IMPACT PROBABILITIES AND VELOCITY DISTRIBUTIONS

To create an accurate crater probability distribution for the Earth and the Moon, separate impact probabilities and velocity distributions have been used for each NEO population. It is important to include these parameters for each contributory population, as they determine the resulting crater diameter and the frequency of impact.

2.1 Collision code

The Öpik (1951, 1976) based geometric algorithm of Manley, Migliorini & Bailey (1998) has been used to calculate the collisional probability per unit time between objects moving in arbitrary elliptical orbits. The algorithm is an adaptation of the Wetherill (1967) and Greenberg (Bottke & Greenberg 1993) methods, and avoids a number of approximations made by Öpik. Objects are assumed to be spherical and small compared with the size of their orbits. Also included is gravitational focusing for encounters with large bodies such as planets.

[★]E-mail: meb@star.arm.ac.uk

The collision code is particularly suitable for determining impact probabilities for populations of bodies in which the argument of perihelion ω and the longitude of the ascending node Ω take random, uniformly distributed values in the range $(0, 360^\circ)$. The code explores all possible values of ω and Ω , taking as input the semi-major axis a , eccentricity e and inclination i of the colliding objects.

Accounting for the Moon's orbit around the Earth introduces a correction arising from the gravitational field of the Earth of approximately 1.4 km s^{-1} , and an additional velocity component of approximately 1 km s^{-1} . This velocity component is randomly distributed in the plane of the Earth's orbit, ignoring the small inclination of the Moon's orbit to the ecliptic.

As the Moon orbits the Earth at a distance of 0.0026 au , it is necessary also to take account of the variation of the Moon's heliocentric distance. This is modelled by increasing the eccentricity of the target orbit (in this case the Moon). This does not accurately take account of the true geometry, since the extrema in heliocentric distance only occur when the Moon has a particular configuration. However, since the collision algorithm itself involves various approximations, further minor improvements are not justified at this time.

These factors lead to a small difference in the impact velocity distributions between the Earth and the Moon beyond that arising from the difference in their respective gravitational attractions. This is an important extension of the algorithm, enabling it to be used also for impacts on satellites of other bodies (e.g. the Martian, Jovian and Saturnian systems). We have not implemented further possible refinements of the model, for example considering the varying terrestrial eccentricity over astronomical time-scales.

2.2 Velocity distributions on the earth and the moon

The four component NEO populations considered are near-Earth asteroids (NEAs), short-period comets (SPCs), Halley-type comets (HTCs) and long-period comets (LPCs).

In order to overcome the effects of observational bias associated with NEAs (a few observed objects of low inclination with extremely high collision probabilities at low velocity), a synthetic distribution of orbital elements for 20 000 asteroids has been calculated. This uses the probability distribution in a , e and i of Rabinowitz et al. (1994), and a Monte Carlo (MC) numerical method.

LPCs, i.e. comets with periods $P > 200 \text{ yr}$, were modelled using an MC simulation based on an assumed isotropic parabolic source distribution. The same procedure is not applied to the distributions of SPCs (with $P < 20 \text{ yr}$) and HTCs (which we define as $20 < P < 200 \text{ yr}$; but see discussion later), as they are not well modelled by an isotropic source population. Instead, the populations of SPCs and HTCs are derived from Shoemaker, Weissman & Shoemaker (1994) and Emel'yanenko & Bailey (1998).

The frequency distributions of impact velocities are plotted for each component NEO population in Fig. 1, for the Earth and Moon respectively. Each panel indicates the total population of bodies estimated to exist (Pop), the mean impact probability per object (MIP), the total impact probability (TP) from the assumed population, i.e. $\text{Pop} \times \text{MIP}$, and the mean impact velocity (MIV). The quantity Pop depends on the assumed minimum size of object in the population (see Section 3.2).

For NEAs, the mean impact probabilities with respect to the Earth computed by Shoemaker, Wolfe & Shoemaker (1990) and

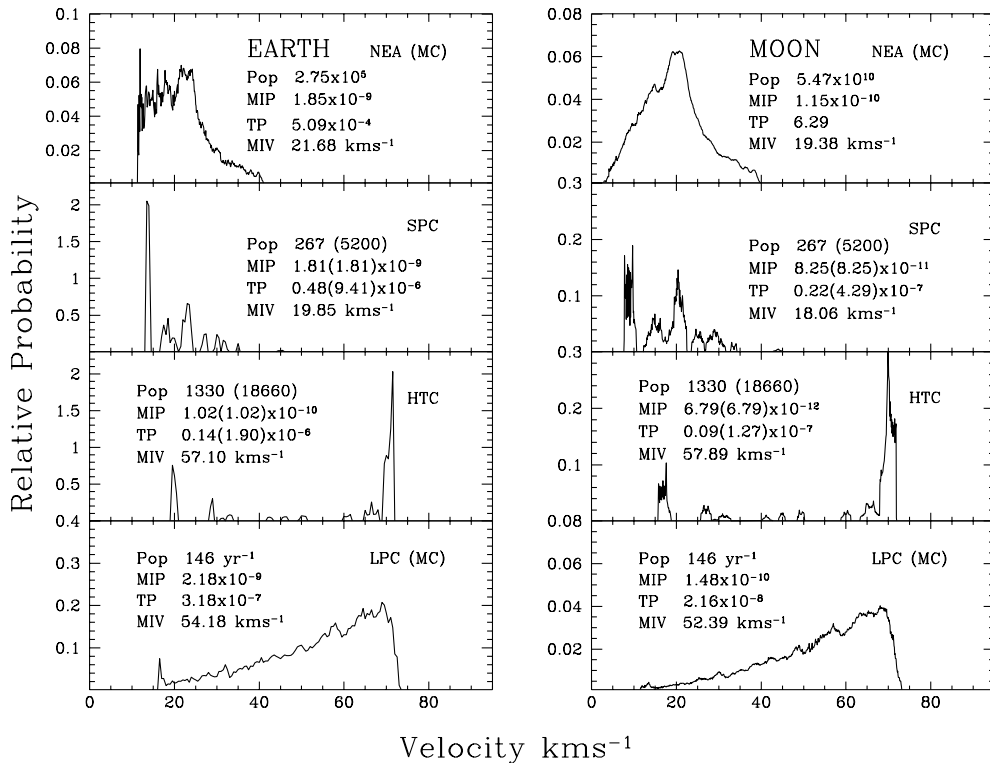


Figure 1. Velocity distributions for NEAs, SPCs, HTCs and LPCs impacting the Earth. The normalized probabilities (per unit velocity interval) have a velocity resolution of 0.1 km s^{-1} . Pop denotes the total number of bodies estimated to exist in the population (for SPCs and HTCs the first number denotes active comets and the second the number of inactive bodies), MIP is the mean impact probability per object per year (per revolution for LPCs), TP is the total impact probability (yr^{-1}) and MIV is the mean impact velocity.

Steel (1998), 4.2×10^{-9} and 5.08×10^{-9} $\text{object}^{-1} \text{yr}^{-1}$ respectively, are higher than our value (1.85×10^{-9} $\text{object}^{-1} \text{yr}^{-1}$). This is because the previous calculations were for observed asteroids, therefore biasing the results towards objects currently in orbits passing close to Earth.

The results for LPCs are in good agreement with those of other authors such as Steel (1998) and Weissman (1997), who respectively found values of 2.2×10^{-9} and $2.2\text{--}2.5 \times 10^{-9}$ per revolution. Results using *observed* LPCs are slightly higher (3.5×10^{-9} per revolution: Shoemaker 1984; Manley et al. 1998), because the observed LPC *i*-distribution is not quite so isotropic, and there is a bias due to observed objects with perihelion distances close to 1 au and a handful of objects with inclinations close to zero or 180° (Steel 1993).

The velocity distributions for the SPCs and HTC appear somewhat fragmented, a result of the small number of objects used in each case to generate the distributions. The NEA and LPC populations display a smoother velocity distribution because they originate from much larger synthetic populations.

The mean impact probabilities for the Moon are generally lower than those on the Earth. This is particularly noticeable for populations with low encounter velocities, e.g. NEAs, as the stronger gravitational potential of the Earth is then more significant. In the case of the Moon, 10 per cent of NEAs impact at less than 10 km s^{-1} , compared with none for the Earth, the differences in the shapes of the two distributions being clear. The sharp peak at the lower end of the frequency distribution of SPC (and to a lesser extent HTC) impactors demonstrates the existence of comets with relatively low impact velocities. Whereas the HTC velocity distributions are comparable for the Earth and the Moon, the difference between prograde and retrograde orbits leads to a bimodality of the two curves.

An important feature is the generally higher impact velocity associated with the majority of bodies in cometary orbits compared with those of asteroids. This leads to a different degree of gravitational focusing, and also influences the final crater diameter through the velocity dependence of the crater scaling laws (Section 3.1).

3 PREDICTED CRATER SIZE DISTRIBUTION

The crater size distributions, resulting from each NEO population impacting against the Earth and the Moon, have been obtained by combining the impact probabilities and velocity distributions with a range of crater scaling laws and the size distribution of the relevant NEO population.

3.1 Crater diameter scaling

A review of the literature indicates a proliferation of different crater scaling laws. Table 1 lists eight of these laws which have been selected from a list of 17 (Jeffers 2000), and converted into a general form of equation (1):

$$\log D_t = k + k_v \log v_i + k_d \log d_i + k_{\rho_i} \log \rho_i + k_{\rho_t} \log \rho_t + k_g \log g_t + k_\theta \log \cos \theta. \quad (1)$$

Here D_t denotes the resulting transient or initial crater diameter (m), v_i the impactor velocity (m s^{-1}) and d_i the impactor diameter (m). The constant input parameters for this analysis are as follows: ρ_i (the impactor density) is 2000 and 1000 kg m^{-3} (Harmon et al. 1999) for asteroids and comets respectively; for the Earth and the Moon respectively ρ_t (the target density) is 2600 and 2400 kg m^{-3} and g_t (the surface gravity) is 9.81 and 1.62 m s^{-2} . In the simulation, the evaluation of θ (the angle of impact, measured from the vertical) is based on there being an equal flux from equal angular areas for an isotropic source. All units are SI and logarithms are to base 10. The corresponding constants, k , k_v , k_d , k_{ρ_i} , k_{ρ_t} , k_g and k_θ , are tabulated in Table 1.

3.2 NEO size distribution: asteroids and comets

The NEA size distribution adopted in this analysis is that of Rabinowitz et al. (1994) and Moore et al. (1980) for impactors $> 10 \text{ m}$ and $< 10 \text{ m}$ in diameter, respectively. The size distribution of Rabinowitz et al. has been chosen as it also includes an orbital element probability distribution from which it is possible to simulate the MC distribution of NEAs used in the previous section. The size distribution of Moore et al. has been chosen because it is valid for small sizes that are generally not included in other laws primarily because an extrapolation may be misleading. In agreement with Moore et al. (1980), the fireball data of Ceplecha (1988) would suggest that the power-law index of the cumulative size distribution decreases for asteroids with diameters $< 5 \text{ m}$. The size distributions of Rabinowitz et al. (1994) and Moore et al. (1980) are tabulated below. The uncertainty that applies to this size distribution is believed to be less than a factor of 2 for 1-km asteroids.

$$N(> d) \propto d^{-\alpha} \begin{cases} \alpha = 2.34, & 0.001 < d < 0.010 \text{ km}, \\ \alpha = 3.5, & 0.010 < d < 0.070 \text{ km}, \\ \alpha = 2.0, & 0.07 < d < 3.5 \text{ km}, \\ \alpha = 5.4, & 3.5 \text{ km} < d. \end{cases} \quad (2)$$

In the case of the Earth, NEAs down to $d = 70 \text{ m}$ are considered, a total of 2.75×10^5 objects in the above distribution. This is

Table 1. Parameters for various crater scaling laws. The parameters are as presented in equation (1).

No.	Source	Scaling law parameters						
		k	k_v	k_d	k_{ρ_i}	k_{ρ_t}	k_g	k_θ
1	Melosh (1989)	-0.091	0.440	0.790	0.330	-0.330	0.0	0.0
2	Moore, Boyce & Hahn (1980)	-1.446	0.555	0.833	0.278	0.0	0.0	0.0
3	Schmidt & Housen (1988)	0.047	0.430	0.780	0.330	-0.330	-0.220	0.0
4	Grieve & Shoemaker (1994)	0.064	0.440	0.780	1/3	-1/3	-0.220	0.0
5	Shoemaker & Wolfe (1982)	-1.733	0.588	0.882	0.588	-0.294	-1/6	0.0
6	Wetherill (1989)	0.169	0.433	0.781	0.336	-0.336	-0.216	0.0
7	Zahnle, Dones & Levison (1999)	0.066	0.440	0.780	0.333	-0.333	-0.220	0.44
8	Dence, Grieve & Robertson (1977) ($D < 2400 \text{ m}$)	-2.398	2/3	1.0	1/3	0.0	-0.188	0.0
		-1.694	0.588	0.882	0.294	0.0	-0.188	0.0

approximately the minimum size for an asteroid capable of reaching the Earth’s surface. In practice, iron asteroids smaller than ~ 70 m may occasionally penetrate the Earth’s atmosphere and make a crater, but they are much smaller in number than the more friable chondrites. NEAs down to $d = 1$ m are included in the case of the Moon, hence the larger total population ‘Pop’ in Fig. 1.

For comets the size distribution of Donnison (1986, 1987), based on an analysis of cometary magnitudes, is followed. It is assumed that a single power law can be used to describe cometary observations. The results of Donnison (1986, 1987) comprise two parts, one power law for LPCs and another for SPCs, indicated below in equation (3). The error that applies to these values is ± 0.15 for LPCs and 0.42 for SPCs, indicating that they could also be consistent both with each other and with the value $\alpha = 2$ (cf. the asteroid law in equation 2).

$$N(> d) \propto d^{-\alpha} \begin{cases} \alpha = 2.13, & \text{LPC,} \\ \alpha = 2.07, & \text{SPC, HTC.} \end{cases} \quad (3)$$

The flux of LPCs within 1 au has been calibrated by Manley (in preparation), where, following the work of Kresák (1978), an orbital distribution for LPCs on Earth-approaching orbits has been derived. A list has been determined of 15 LPCs that had an absolute visual magnitude $H_0 < 7$ (≈ 4 km) and were on an Earth-crossing orbit with impact parameter to the Earth less than 0.2 au, over a period of 300 yr. It is assumed that such objects would not have been missed even using naked eye observational techniques, and

the derived LPC orbital distribution then gives the total flux of Earth-crossing LPCs brighter than $H_0 = 7$.

A lower limit of 0.4 km on the diameter has been imposed on the cometary populations (cf. Fernández et al. 1999). This figure is in agreement with the observations of Lowry et al. (1999) for the smallest possible comet nuclei, based on observed lower limits of nuclear sizes for active comets. The numbers at $d = 1$ km estimated by Shoemaker et al. (1994) and Emel’yanenko & Bailey (1998) are extrapolated to this assumed lower limit to give the overall population sizes. An upper limit of 1000 km is enforced as this is the order of the size of the largest objects in the Edgeworth–Kuiper Belt.

3.3 Frequency distribution of crater diameters

Using appropriate input parameters for any given crater diameter scaling law, it is a simple MC process to generate predicted crater size distributions from any given source population. The probability distributions for the individual NEO populations are then summed, weighting each population by the appropriate normalized impact probability. This results in a total crater size distribution for each crater diameter scaling law, for both the Earth and the Moon.

In order to represent the frequency of asteroid impacts of all sizes, the asteroid size distribution is divided into separate diameter regimes: 1–10 m (5.47×10^{10} asteroids), 10–70 m (2.5×10^8 asteroids) and > 70 m (2.75×10^5 asteroids), the first two

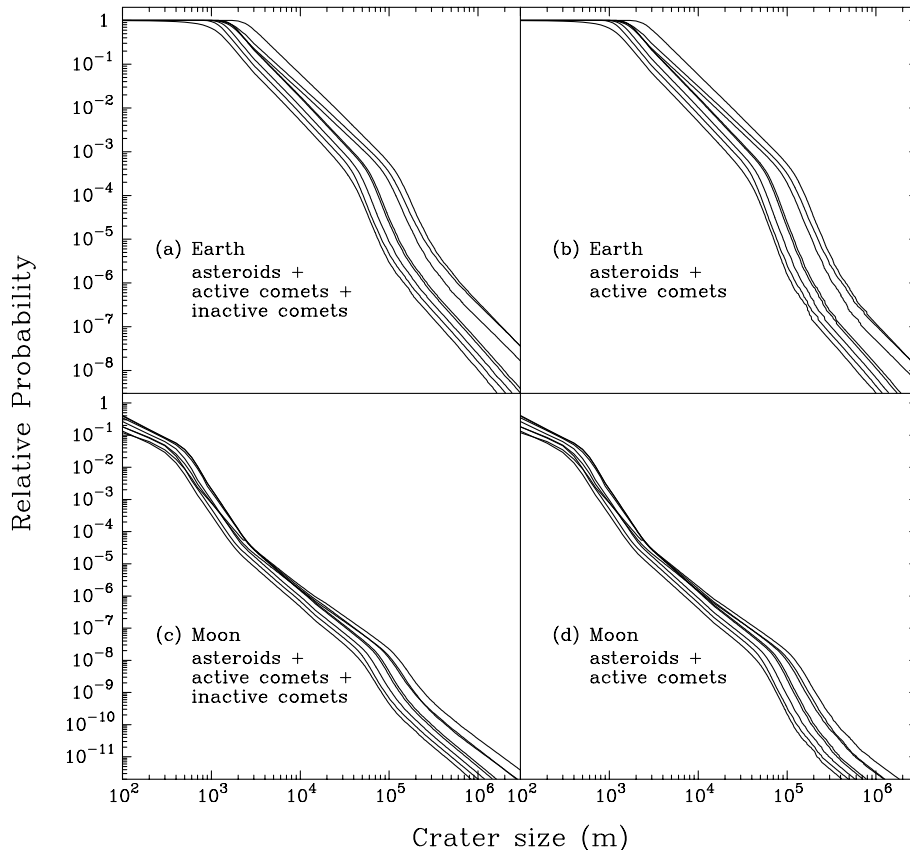


Figure 2. Log–log cumulative plot of relative frequency versus crater diameter, for various crater scaling laws. (a) Earth; (b) Earth excluding inactive comets; (c) Moon; (d) Moon excluding inactive comets. The crater scaling laws are in the following order, at relative probability 10^{-3} : Grieve & Shoemaker (1994), Wetherill (1989), Zahnle et al. (1999), Shoemaker & Wolfe (1982), Melosh (1989), Schmidt & Housen (1988), Moore et al. (1980) and Dence et al. (1977).

ranges applying to the results for the Moon only. It can be seen that the predicted distributions of crater diameters for the Earth and the Moon, Figs 2(a) and (c) respectively, retain strong elements of the size distributions of the underlying populations that generated them. The different velocity distributions generally serve merely to spread the distribution and dilute the dependence on impactor size.

The dependence on the size distribution is illustrated by the presence of a ‘knee’ in the distribution. This occurs at probabilities of about 10^{-3} to 10^{-4} on the Earth and at about 10^{-8} on the Moon, where the number of asteroids with sizes > 3.5 km begins to drop off rapidly. The precipitous drop is halted when the curve catches up with the probability distribution for comets. Here, there is a clear indication of the effects of different populations of contributing bodies, i.e. comets dominate the production rate for large craters on both the Earth and the Moon.

The crater size distribution for the Earth starts with larger craters, as a result of the decision to remove any object with size below 70 m. On the Moon, as the atmosphere does not affect the incoming population, there is an abundance of small craters. This is particularly important for the calibration of these MC results, as statistics for small craters will be far superior to those of the larger craters. In the size range where there are craters on the Earth, the weaker gravitational focusing of the Moon leads to differences in the cratering distributions between the Earth and the Moon. Overall, at a given diameter the cratering rate per unit area is typically ~ 30 per cent less on the Moon.

Excluding the contribution of ‘dark’ inactive comets proposed by Shoemaker et al. (1994), Emel’yanenko & Bailey (1998) and Bailey & Emel’yanenko (1998), Figs 2(a) and (c) now have the appearance of parts (b) and (d), for the Earth and Moon respectively. The resulting effect is that the comets do not begin to make an appearance until lower probabilities are reached.

3.4 Fractional probabilities of iridium deposition

The question of a cometary versus asteroidal nature for the impactor that produced the famous Chicxulub structure has often been debated. The geological evidence is not yet conclusive (Shukolyukov & Lugmair 1998; cf. Kyte 1998), and the physical nature and composition of cometary nuclei are other significant unknowns. The calculations in this paper nevertheless impose constraints on the nature of the impactor. Fig. 2 shows it to be in the comet-dominated size range, and therefore – considering the size of the crater alone – it was probably generated by a comet. However, the associated Ir signature provides an additional piece

of evidence, namely that the object should deposit sufficient mass to match the observed Ir.

In fact, provided that the body is in the multi-kilometre size range, the fraction of the mass of the impactor deposited is a sharply decreasing function of the impactor velocity. From Vickery & Melosh (1990), for silicate impactors with $V \sim 20$ km s $^{-1}$ in the size range of relevance for the K/T Ir layer, the impactor deposits ~ 80 per cent of its original mass. However, impactors with $V \sim 25$ km s $^{-1}$ deposit only 15–20 per cent, i.e. the fraction of the impactor mass that is retained by the Earth drops rapidly as the impact velocity rises through the range 20 to 25 km s $^{-1}$, and above 25 km s $^{-1}$ essentially none of the impactor mass is retained. This means that the initial mass required to explain any given Ir anomaly increases rapidly with increasing impact velocity above 20 km s $^{-1}$.

Thus we assume that impactors arriving at the Earth’s surface with speeds greater than 25 km s $^{-1}$ will not create a significant Ir anomaly, and that impactors arriving at 25 km s $^{-1}$ need to have a diameter 1.6 times greater than those at 20 km s $^{-1}$. Assuming that an asteroid that could generate the K/T Ir layer has a minimum diameter $d \approx 6.6$ km (Alvarez et al. 1980), one with an impact velocity $V \approx 25$ km s $^{-1}$ would have $d \approx 10.5$ km (and hence, other things being equal, would make a much larger crater). Similarly, the minimum size of a cometary impactor would be 8.3 km for $V < 20$ km s $^{-1}$, owing to the lower density of cometary material (cf. Section 3.1). Indeed, one could argue for an even greater increase in the diameter of the cometary nucleus necessary to yield a given amount of Ir, owing to comets containing a smaller proportion of chondritic material (Sharpton & Marín 1997). However, this refinement is omitted in Table 2 below, since the proportion in the various populations of bodies is rather uncertain. We also note that active comets may be relatively richer in ices, at the expense of chondritic material, compared with extinct comets and asteroids.

The numbers of potential impactors at these various sizes can be evaluated from the size distributions of each population (Section 3.2). The fractions of asteroids and comets with an impactor velocity (i) ≤ 20 km s $^{-1}$ and (ii) in the range $20 < V \leq 25$ km s $^{-1}$ can be found from the calculations of Section 2.2, as can the impact probabilities. Thus a fractional probability for the relevant impactor size and velocity ranges has been calculated, equal to the inverse of the impact interval. These probabilities for an impactor to leave sufficient mass to account for the observed Ir layer at the K/T boundary are given in Table 2.

The calculated results confirm that the population of NEAs has a

Table 2. Impact probabilities per year for objects in different orbits with large enough diameters to produce the observed Ir at the K/T boundary. For SPCs and HTC, values are given both for all objects and for active comets. Note that bodies arriving with high impact velocities (> 20 km s $^{-1}$) must be much more massive in order to deposit enough Ir to explain that observed. Such bodies, whether comets or asteroids, are very rare, i.e. the mean impact interval between them is exceptionally long. This indicates a low-velocity impactor (i.e. $V \approx 20$ km s $^{-1}$).

Velocity Object	$V \leq 20$			$20 < V \leq 25$			Total ($V \leq 25$)	
	Min d (km)	Fraction prob yr $^{-1}$	Impact interval	Min d (km)	Fraction prob yr $^{-1}$	Impact interval	Fraction prob yr $^{-1}$	Impact interval
NEA	6.6	3.290×10^{-9}	304×10^6	10.5	1.508×10^{-10}	6.63×10^9	3.441×10^{-9}	290×10^6
SPC(all)	8.3	1.050×10^{-8}	95.3×10^6	13.2	6.694×10^{-10}	1.49×10^9	1.117×10^{-8}	89.6×10^6
SPC(act)	8.3	5.095×10^{-10}	1.96×10^9	13.2	3.236×10^{-11}	30.9×10^9	5.419×10^{-10}	1.85×10^9
HTC(all)	8.3	3.425×10^{-11}	29.2×10^9	13.2	1.723×10^{-11}	58.0×10^9	5.148×10^{-11}	19.4×10^9
HTC(act)	8.3	2.277×10^{-12}	439×10^9	13.2	1.149×10^{-12}	871×10^9	3.426×10^{-12}	292×10^9
LPC	8.3	9.994×10^{-12}	100×10^9	13.2	4.385×10^{-12}	228×10^9	1.438×10^{-11}	69.5×10^9

substantial probability of generating the Ir anomaly as a result of their low velocities, as was found by Vickery & Melosh (1990). However, Table 2 also shows that this group is more than matched by inactive SPCs, with a mean interval to generate an equivalent Ir signature of approximately 100 Myr. The HTCs and LPCs have essentially zero probability of depositing sufficient mass to generate the K/T anomaly, and the velocity distributions therefore strongly argue against the K/T impactor coming directly from either of these populations.

4 DISCUSSION

Was the Chicxulub event caused by a low-velocity comet or a rare, large asteroid? On the one hand, comets are the main source of the largest terrestrial and lunar impact craters, as they have generally larger sizes and higher impact velocities than NEAs. However, their large impact velocities ($\geq 25 \text{ km s}^{-1}$) make them poor candidates for depositing significant amounts of Ir. Therefore, whilst the lack of Ir (or other siderophile elements) at geological boundaries does not rule out impacts as the cause of extinctions, its presence at the K/T boundary would seem to strengthen the asteroidal hypothesis.

Moreover, Kyte (1998) has presented evidence for a fossil meteorite in deep sea sediments associated with the K/T boundary layer, arguing for an asteroidal origin for the impactor. However, the internal structure and composition of a comet (or comet fragment) capable of producing the K/T event are not known, and the dynamical process of transport from the main belt to the NEA region would favour smaller bodies, more boulder-like than large asteroids. A 6.6-km asteroid fragment would be unlikely to gain the necessary velocity from a collision to be ejected directly into a resonance from the dynamically stable main belt, and would have to be transported by long-term secular processes (e.g. Menichella, Paolicchi & Farinella 1996; Zappalà et al. 1998; Farinella, Vokrouhlický & Hartmann 1998).

The difficulty of dynamically transporting a sufficiently large asteroid from the main belt on to an Earth-crossing orbit suggests that a comet, possibly assisted by outgassing (Öpik 1963; Harris & Bailey 1998; Asher, Bailey & Steel 2001) should be considered as an alternative candidate for the K/T impactor. A cometary hypothesis would be consistent with the arguments of Zahnle & Grinspoon (1990), and by the geological evidence for prolonged environmental change on either side of the K/T boundary (e.g. Bailey et al. 1994).

Such a near-Earth object might have been an active Jupiter-family comet (JFC), but more probably would have been an inert or devolatilized object, perhaps originating from a JFC orbit (cf. 2P/Encke), or from the HTC population (cf. 96P/Machholz 1). The latter object has $P \sim 5.25$ yr, and hence an SPC classification according to the scheme of this paper, but dynamical characteristics closer to the Halley family (cf. classifications involving the Tisserand parameter: Carusi et al. 1987; Levison & Duncan 1997), indicating an origin in the Oort Cloud.

Favouring an Oort Cloud connection is the argument that geological disturbances arise periodically at approximately 30-Myr intervals following passages of the Solar system through the Galactic plane (e.g. Smoluchowski, Bahcall & Matthews 1986). To be detectable, enhancements in the cometary collision rate with the Earth would need to be strong compared with the background level of asteroid impacts from the main belt. However, if a ~ 30 -Myr cycle of mass extinctions is accepted, then further investigations into the evolution of Oort Cloud comets captured

into SPC orbits and their wider geological effects would be merited.

Fluctuations in the NEO population are also expected to occur stochastically, for example following the close passage of a star through the Oort Cloud (Hills 1981) or an exceptional collision in the main asteroid belt (Kortenkamp & Dermott 1998; Zappalà et al. 1998). Each of these scenarios would lead to a substantial short-term (10^5 – 10^6 yr) increase in the comet or asteroid population in near-Earth space, accompanied by a significantly increased abundance of interplanetary dust which would be accreted by the Earth over a similar time-scale. Such a picture is consistent with ^3He data from interplanetary dust associated with the late Eocene (Farley 1995; Farley et al. 1998), but not with the K/T boundary (Mukhopadhyay, Farley & Montanari 2001). The latter have argued for a one-off asteroid impact or a lone comet, and against there being a significant enhancement of the comet/asteroid population in near-Earth space at this time.

Finally, we note that various alternative sources of K/T Ir, not directly associated with the Chicxulub impactor, have also been proposed. Clube & Napier (1984) have pointed out that a large disintegrating comet may substantially enhance the stratospheric dust load through intense bombardment by ‘Tunguska-sized’ sub-kilometre meteoroids (cf. Napier 2001). A similarly enhanced rate of dust accretion at the K/T boundary with a time-scale of the order of 10^5 yr, associated with the evolution of a giant comet, has been independently proposed by Zahnle & Grinspoon (1990). Scenarios in which the K/T Ir is not directly associated with the Chicxulub impactor would require the latter to have a moderate to high impact velocity, strengthening the argument for a cometary provenance.

A quite different hypothesis for the K/T Ir excess has been proposed by Yabushita & Allen (1997), namely that the Earth encountered a dense molecular cloud ~ 65 Myr ago. However, no isotopic anomalies attributable to interstellar material have yet been detected at the K/T boundary.

5 CONCLUSIONS

The principal conclusions of this paper are as follows:

- (i) the presence of a strong iridium signature, if associated with the Chicxulub crater, suggests that the K/T projectile had an impact velocity $V \lesssim 20 \text{ km s}^{-1}$ (Vickery & Melosh 1990), and therefore cannot have been a Halley-type or long-period comet;
- (ii) the presently observed number of comets and asteroids on Earth-crossing orbits, together with the large size of the crater, suggests that the projectile was most probably a devolatilized or inert short-period comet ($P < 20$ yr); and
- (iii) such a body could have evolved from the Jupiter-family, Halley-type or long-period populations, leaving open the question of its ultimate source, whether in the Edgeworth–Kuiper Belt or the Oort Cloud.

ACKNOWLEDGMENTS

We thank Alan Fitzsimmons (Queen’s University Belfast) for helpful discussions during the course of this work, and Duncan Steel (University of Salford) and Bill Napier for suggestions to improve and clarify the paper. This research was supported by the Irish Department of Education, the NI Department of Culture, Arts

and Leisure, and the Particle Physics and Astronomy Research Council.

REFERENCES

- Alvarez L., Alvarez W., Asaro F., Michel H., 1980, *Sci*, 208, 1095
- Asher D. J., Bailey M. E., Steel D. I., 2001, in Marov M., Rickman H. eds, *Collisional Processes in the Solar System*. *Astrophys. Space Sci. Lib.*, Vol. 261. Kluwer, Dordrecht, in press
- Bailey M. E., Emel'yanenko V. V., 1998, in Grady M. M., Hutchison R., McCall G. J. H., Rothery D. A. eds, *Geol. Soc. Spec. Publ. No. 140*, *Meteorites: Flux with Time and Impact Effects*. The Geological Society, London, p. 11
- Bailey M. E., Clube S. V. M., Hahn G., Napier W. M., Valsecchi G. B., 1994, in Gehrels T. ed., *Hazards due to Comets and Asteroids*. Univ. Arizona Press, Tucson, p. 479
- Bottke W. F., Greenberg R., 1993, *Geophys. Res. Lett.*, 20, 879
- Carusi A., Kresák Ľ., Perozzi E., Valsecchi G. B., 1987, *A&A*, 187, 899
- Ceplecha Z., 1988, *Bull. Astron. Inst. Czech.*, 39, 221
- Clube S. V. M., Napier W. M., 1984, *MNRAS*, 211, 953
- Dence M. R., Grieve R. A. F., Robertson P. B., 1977, in Roddy D. J., Pepin R. O., Merill R. B. eds, *Impact and Explosion Cratering*. Pergamon, New York, p. 137
- Donnison J. R., 1986, *A&A*, 167, 359
- Donnison J. R., 1987, *Earth, Moon, Planets*, 38, 263
- Emel'yanenko V. V., Bailey M. E., 1998, *MNRAS*, 298, 212
- Farinella P., Vokrouhlický D., Hartmann W. K., 1998, *Icarus*, 132, 378
- Farley K. A., 1995, *Nat*, 376, 153
- Farley K. A., Montanari A., Shoemaker E. M., Shoemaker C. S., 1998, *Sci*, 280, 1250
- Fernández J. A., Tancredi G., Rickman H., Licandro J., 1999, *A&A*, 352, 327
- Grieve R. A. F., Shoemaker E. M., 1994, in Gehrels T. ed., *Hazards due to Comets and Asteroids*. Univ. Arizona Press, Tucson, p. 417
- Harmon J. K., Campbell D. B., Ostro S. J., Nolan M. C., 1999, *Planet. Space Sci.*, 47, 1409
- Harris N. W., Bailey M. E., 1998, *MNRAS*, 297, 1227
- Hills J. G., 1981, *AJ*, 87, 906
- Jeffers S. V., 2000, MPhil thesis The Queen's University of Belfast
- Kortenkamp S. J., Dermott S. F., 1998, *Sci*, 280, 874
- Kresák Ľ., 1978, *Bull. Astron. Inst. Czech.*, 29, 103
- Kyte F. T., 1998, *Nat*, 396, 237
- Levison H. F., Duncan M. J., 1997, *Icarus*, 127, 13
- Lowry S. C., Fitzsimmons A., Cartwright I. M., Williams I. P., 1999, *A&A*, 349, 649
- Manley S. P., Migliorini F., Bailey M. E., 1998, *A&AS*, 133, 437
- Melosh H. J., 1989, *Oxford Monographs on Geology and Geophysics*, No. 11, *Impact Cratering: A Geologic Process*. Oxford Univ. Press, Oxford
- Menicella M., Paolicchi P., Farinella P., 1996, *Earth, Moon, Planets*, 72, 133
- Moore H. J., Boyce J. M., Hahn D. A., 1980, *Moon & Planets*, 23, 231
- Mukhopadhyay S., Farley K. A., Montanari A., 2001, *Sci*, 291, 1952
- Napier W. M., 2001, *MNRAS*, 231, 463
- Öpik E. J., 1951, *Proc. R. Ir. Acad.*, 54, 165
- Öpik E. J., 1963, *Adv. Astron. Astrophys.*, 2, 219
- Öpik E. J., 1976, *Interplanetary Encounters: Close Range Gravitational Interactions*. Elsevier Scientific Publ., Amsterdam
- Rabinowitz D., Bowell E., Shoemaker E., Muinonen K., 1994, in Gehrels T. ed., *Hazards due to Comets and Asteroids*. Univ. Arizona Press, Tucson, p. 285
- Schmidt R. M., Housen K. R., 1988, *Global Catastrophes in Earth History*, *Snowbird Abstracts*, LPI Contrib. No. 973 (NASA CR-183329, N89-21381). NASA, Washington DC, p. 162
- Sharpton V. L., Marín L. E., 1997, *Ann. NY Acad. Sci.*, 822, 353
- Shoemaker E. M., 1984, in Holland H. D., Trendall A. F. eds, *Patterns of Change in Earth Evolution*. Springer-Verlag, Berlin, p. 15
- Shoemaker E. M., Wolfe R. F., 1982, in Morrison D. ed., *Satellites of Jupiter*. Univ. Arizona Press, Tucson, p. 277
- Shoemaker E. M., Wolfe R. F., Shoemaker C. S., 1990, in Sharpton V. L., Ward P. D. eds, *Geol. Soc. Am. Spec. Paper 247*, *Global Catastrophes in Earth History: An Interdisciplinary Conference on Impacts, Volcanism, and Mass Mortality*. The Geological Society of America, Boulder, p. 155
- Shoemaker E. M., Weissman P. R., Shoemaker C. S., 1994, in Gehrels T. ed., *Hazards due to Comets and Asteroids*. Univ. Arizona Press, Tucson 313
- Shukolyukov A., Lugmair G. W., 1998, *Sci*, 282, 927
- Smoluchowski R., Bahcall J. N., Matthews M. S. eds, 1986, *The Galaxy and the Solar System*. Univ. Arizona Press, Tucson
- Steel D. I., 1993, *MNRAS*, 264, 813
- Steel D., 1998, *Planet. Space Sci.*, 46, 473
- Vickery A. M., Melosh H. J., 1990, in Sharpton V. L., Ward P. D. eds, *Geol. Soc. Am. Spec. Paper 247*, *Global Catastrophes in Earth History: An Interdisciplinary Conference on Impacts, Volcanism, and Mass Mortality*. The Geological Society of America, Boulder, p. 289
- Weissman P. R., 1997, *Ann. NY Acad. Sci.*, 822, 67
- Wetherill G. W., 1967, *J. Geophys. Res.*, 72, 2429
- Wetherill G. W., 1989, *Meteoritics*, 24, 15
- Yabushita S., Allen A., 1997, *Astron. Geophys.*, 38, 2, 15
- Zahnle K., Grinspoon D., 1990, *Nat*, 348, 157
- Zahnle K., Dones L., Levison H., 1999, *Icarus*, 136, 202
- Zappalà V., Cellino A., Gladman B. J., Manley S., Migliorini F., 1998, *Icarus*, 134, 176

This paper has been typeset from a \TeX/L\AA\TeX file prepared by the author.